Adsorption of iodine and potassium on $Bi_2Sr_2CaCu_2O_{8+\delta}$ investigated by low-energy alkali-ion scattering

R. D. Gann,[1] J. X. Cao,[2] R. Q. Wu,[2] Jinsheng Wen,[3] Zhijun Xu,[3] G. D. Gu,[3] and J. A. Yarmoff[1,*]

[1]*Department of Physics, University of California, Riverside, California 92521, USA*

[2]*Department of Physics, University of California, Irvine, California 92697, USA*

[3]*Condensed Matter Physics & Materials Science Department, Brookhaven National Laboratory, Upton, New York 11973, USA*

(Received 15 October 2009; revised manuscript received 15 December 2009; published 20 January 2010)

The adsorption of K and I on the surface of the high-T_c cuprate BSCCO-2212 is investigated with low-energy (0.8 to 2 keV) Na^+ ion scattering and density functional theory (DFT). Samples were cleaved in ultrahigh vacuum and charge-resolved spectra of the scattered ions were collected with time-of-flight. The spectra contain a single peak representing Na scattered from Bi, as the clean surfaces are terminated by BiO. The neutralization of scattered Na depends on the local potential above the target site, and the angular dependence indicates that the clean surface has an inhomogeneous potential. Neutralization is dependent on the coverage of I, but independent of K adsorption. DFT suggests high-symmetry sites for the adsorption of both I and K, and that the potential above the Bi sites is altered by I by an amount consistent with the experimental findings, while the potential is not affected by K adsorption. DFT also enables an experimental determination of the "freezing distance," which is the effective point beyond which charge exchange does not occur, to be 1.6 ± 0.1 Å from the outermost Bi layer.

DOI: 10.1103/PhysRevB.81.035418 PACS number(s): 68.43.Fg, 68.47.Gh, 68.49.Sf, 74.25.−q

I. INTRODUCTION

The high-temperature superconducting cuprates are oxides with complex layered structures. Surface studies of these materials are valuable, as they allow for the superconducting cuprate layer to be probed in a detailed way, especially with regard to formation of the paired carriers. One of the materials most often used for surface studies is $Bi_2Sr_2CaCu_2O_8$ (BSCCO-2212), owing to the ease in cleaving the samples in ultrahigh vacuum (UHV), which produces clean terraces of BiO. Previous studies, however, have been mainly confined to scanning probe microscopy and photoemission.[1–3] Reports of ion beam experiments on cuprate materials that do exist have either focused on disorder-induced changes to the critical current,[4] rather than surface physical and electronic structure, or have been on surfaces that are much less ordered than cleaved BSCCO, such as $YBa_2Cu_3O_{7-x}$.[5]

Low-energy ion scattering (LEIS) can provide complementary information to other surface analysis techniques.[6] The method is extremely surface sensitive, as the spectra display peaks resulting from single binary collisions between incident ions and the outermost surface atoms. LEIS can be used to determine composition, surface structure, and, under certain conditions, the local electrostatic potential (LEP). Time-of-flight spectroscopy with alkali-ions, in particular, can simultaneously measure the mass of the surface atoms and the LEP.[7] An incoming alkali-ion has an ionization level typically between 4.3 and 5.4 eV, which is commensurate with the work function at the surfaces of many materials. As the projectile approaches a surface, this ionization level shifts due to the image potential, such that it passes the Fermi energy, and broadens due to overlap of the ion and surface wave functions. The charge-transfer process is nonadiabatic and the final charge state distribution is determined along the outgoing trajectory as the projectile passes through an effective "freezing distance." This makes the neutralization probability of scattered ions a sensitive measure of the local potential just above the scattering site. Results from this method can be interpreted within the well-established theoretical framework of resonant-charge transfer (RCT), which includes both analytical formulas and numerical calculations.[8] Extensive prior experimental work with alkali-ion scattering from metals, along with some work done with simple oxide surfaces (e.g., CeO_2 and TiO_2), provides the context for interpreting the results, and allows some extension of the theory to nonmetals

The RCT framework helps to determine the kinds of measurements to perform when characterizing a system with low-energy alkali-ion neutralization. Theoretical work using a semiclassical approach based on the Anderson Hamiltonian[8,9] shows that the incoming vacant level broadens in energy. The expectation value of the neutralization probability far from the surface, $\langle n(z=\infty)\rangle$, depends principally on the alignment of this level with the Fermi energy at the so-called freezing distance, $z_{fr}=\ln(2\Delta_0/\alpha v_\perp)/\alpha$, where $v_\perp$ is the perpendicular component of the outgoing velocity. This is because the tunneling rate is peaked at this distance, constituting a majority of the tunneling involved in the neutralization process. Because this expression contains $v_\perp$, a strong dependence of neutralization on the outgoing perpendicular velocity is expected, which can be realized either through changing the incident ion energy or through changing the exit angle of the scattered ions. At a fixed energy and exit angle, the neutralization is then sensitive to changes in the surface work function, or more explicitly on the LEP above the scattering site.[10]

In this paper, we present several related measurements in which LEIS was used to investigate the surface of BSCCO. Because the surface is terminated with a Bi-O layer, the principal scattering trajectory involves a single collision with Bi. Results show an angular dependence of the neutralization

 ©2010 The American Physical Society

probability in scattering from the clean surface that reveals an inhomogeneous potential similar to that of other oxide surfaces. It was not possible, for reasons discussed below, to see directly the effect on neutralization by paired carriers. Adsorbed ionic species, potassium and iodine, reside in different bonding sites, significantly influencing the neutral fraction of Na scattered from Bi in the presence of I, but not with K. This result is in agreement with the high-symmetry adsorption site and local potential that are predicted by density functional theory (DFT). In addition, DFT enables an experimental estimate of the freezing distance. We note that, to our knowledge, this is the first time that the RCT model of neutralization in LEIS has been interpreted using DFT.

II. EXPERIMENTAL PROCEDURE

Low-energy alkali-ion scattering experiments were performed in a custom-built UHV chamber. The base pressure was typically 3×10^{-10} torr. Details of the surface analysis equipment and time-of-flight (TOF) instrumentation are described elsewhere.[10] Briefly, a pulsed beam of Na^+ ions is focused onto the sample, and the time differences between the ion pulses and counts recorded on a microchannel plate detector are collected, giving the TOF spectrum. Although the instrument is capable of producing pulse widths as short as 20 ns, a pulse width of ~200 ns was used in this study, which resulted in a large, well-resolved scattered particle peak with good statistics. The detector leg is equipped with deflection plates capable of filtering scattered ions, so that the system can alternately measure the total yield and the yield of neutrals only. In order to account for any long-term drifts in incident beam current during this period, data were collected by cycling between totals and neutrals every 60 s for a scan that took about 30 min in total. Although the scattering angle is fixed at ~150°, the sample can be rotated to change the angle between the surface normal and the detector, and hence change the perpendicular component of the velocity of the exiting projectile.

Float-zone grown single crystals of $Bi_2Sr_2CaCu_2O_{8+\delta}$ were cleaved *in situ* at low temperature by a method detailed elsewhere.[11] Experiments were conducted over the course of a few hours while maintaining the sample at low temperature, although no qualitative difference was observed in the spectra when the samples were heated to room temperature. Maintaining low temperature while taking data was done so that results were comparable to previous scanning tunneling microscopy (STM) work, where almost all samples were cleaved at low temperature and kept cold (cf. Refs. 1–3). Damage due to the incident alkali-ion beam is of concern, particularly in experiments where alkalis themselves are the adsorbate, so the total fluence on any one part of the sample was limited to less than 1 ion per 100 surface atoms. Data were collected with incident energies from 800–3000 eV and several emission angles.

Potassium was deposited from a well-degassed SAES getter, while iodine was deposited from a solid-state AgI electrochemical cell that emits I_2 molecules.[12] X-ray photoelectron spectroscopy confirmed the presence of I on the sample after deposition. The change in surface work function upon deposition was determined via the shift of the low-energy secondary electron cutoff. Secondary electrons were produced by bombarding the sample with a 200 eV electron beam, and the cutoff was measured using a hemispherical electrostatic analyzer (Comstock).[13] The incident electron current during this measurement was approximately 200 nA, and no appreciable changes in the spectra were observed due to electron beam damage during a scan of about 60 s. The sample was exposed to the K or I adsorbates until there was no further change to the work function, thus indicating that saturation coverage was reached.

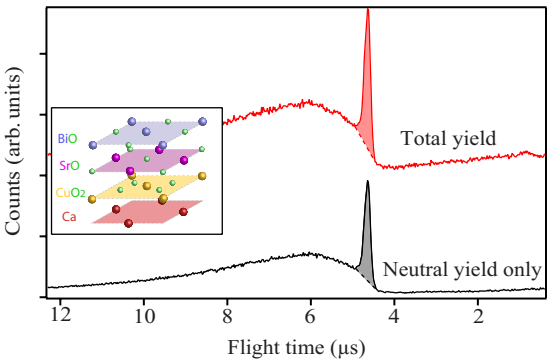

FIG. 1. (Color online) Time-of-flight spectra of 2 keV Na^+ scattered from BSCCO cleaved at 82 K, which shows a pronounced single-scattering peak from Bi. Because of the relatively large background, we employ a background subtraction scheme to calculate the neutralization probability, as shown by the shaded area. Inset: schematic of the first four layers of BSCCO (one inversion).

III. RESULTS AND DISCUSSION

Time-of-flight results for a pristine BSCCO-2212 surface

Figure 1 displays representative charge-resolved TOF ion scattering spectra of 2 keV Na^+ collected from the as-cleaved BSCCO surface. The sharp single-scattering peak (SSP) represents a classical binary collision of Na^+ with a surface Bi atom. No single scattering from oxygen in the outermost layer occurs, since O has a lower mass than the projectile. Single-scattering events from the other constituents of the material are not observed on a virgin surface, presumably due to their being positioned below the surface atoms, and as such being completely shadowed by surface Bi or O. The broad background at longer flight times corresponds to projectiles that have escaped the surface after suffering multiple collisions. This result confirms that the cleaved BSCCO surface is terminated by a BiO plane (illustrated in the inset to Fig. 1), where weak van der Waals binding between the adjacent BiO layers ensures that samples almost always cleave at this interface.[14] The absence of scattering from the deeper lying metal atoms was consistent with a computation of the shadow cones using the empirical formula of Ref. 15 and assuming a simple bulk termination of the structure.

The shaded regions in Fig. 1 illustrate how the area of the SSP was typically resolved from that of the multiple-scattering background. The area of the neutral yield SSP divided by the area of the total yield SSP gives the neutral

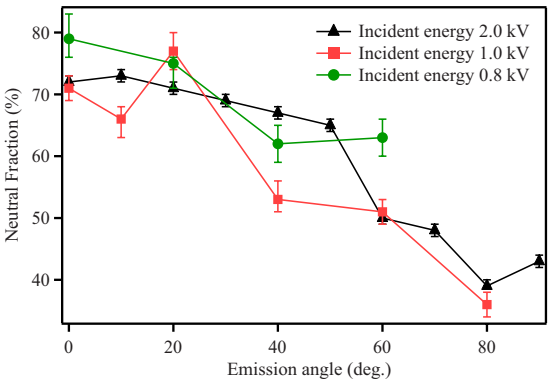

FIG. 2. (Color online) Neutralization versus emission angle for three different incident energies, along with error bars (1 std. dev.). There is at most a marginal dependence on incident energy, with a downward trend as emission angle is increased (corresponding with a lower perpendicular velocity). Note that a pronounced change is not necessarily expected when the energy is varied, as the range of energies for which reliable data could be collected in this case was only within the small range from about 1–2 keV.

fraction for a given sample preparation, incident ion energy and orientation. In determining the error associated with each neutral fraction, both the shot noise, via the square root of the number of integrated counts, and the uncertainty in the time limits of integration are taken into account. The latter is accounted for by recalculating the neutral fraction at slightly different limits of integration, both for the lower and upper limits, and taking the largest and smallest values of the neutral fraction calculated. This is done because the chosen boundaries of the SSP are set visually and are thus somewhat arbitrary. Although variations in beam current are not directly accounted for in the error estimate, totals and neutrals were collected alternatively during each scan, as described above, and the beam current is typically quite stable over the duration of one scan.

Figure 2 shows neutral fractions obtained from a virgin surface at low temperature as a function of emission angle, measured from the surface normal, for three different incident energies. The three energies show identical neutral fractions, within the error bars of the measurement, as the energy range for which good spectra could be obtained is relatively small. Neutralization decreases for larger exit angles.

Note that a significant difference in neutralization was not observed when the data were collected at $T<T_c$ versus $T>T_c$. Although high-T_c materials have an emergent pairing gap at temperatures somewhat above T_c and a condensing of pairs below T_c, the scale of this energy change makes it difficult to measure changes to the surface on that order with the LEIS technique, as the energy of the tunneling states would shift on the order of only 1 meV. Typical error in the neutralization measurement is $\sim$1–5%, and a cursory inspection of the literature suggests that work function shifts need to be at least 0.1 eV to produce an altered neutral fraction outside of these error bars (see, e.g., Ref. 16).

Although the lack of sensitivity to the paired carriers is not surprising, the neutralization is sensitive to the surface work function, and the work function is expected to change when cleaved BSCCO is heated to room temperature. Saito *et al.* found the work function of BSCCO to be 4.849 eV at 85 K, and that it rose by about 0.1 eV when the sample was allowed to warm to 130 K.[17] Although we did not monitor the work function while heating, if we assume that the overall work function does indeed change upon heating as reported, the absence of any temperature dependence to the neutralization suggests that the normally emitted Na probes only a local part of the electrostatic potential, namely that around the Bi atoms themselves, and that this potential is unaffected by annealing. The effect of annealing may involve diffusion of oxygen from the bulk to fill in vacancy defects at the surface, which would be consistent both with the positive change in the work function and the insensitivity of the Bi SSP neutral fraction to the temperature.

It is interesting to compare the dependence in parameter space of LEIS from BSCCO with that of a normal metal. In the case of a metal, the neutralization probability depends principally on the component of velocity perpendicular to the sample, $v_\perp$, along the outward trajectory. In particular, neutralization normally increases as $1/v_\perp$, and hence increases with emission angle when the surface has a homogeneous potential.[18] As seen in Fig. 2, however, the opposite appears to be the case with BSCCO.

Previous alkali-ion scattering studies of CeO_2 surfaces performed in our laboratory have produced a similar reduction in neutral fraction at more grazing angles, which were interpreted as resulting from the inhomogeneous potential associated with an ionic oxide surface.[19] At electropositive sites on a surface, the local work function would be reduced, pushing the Fermi energy up relative to the ionization level and leading to increased neutralization of scattered alkali-ions. Conversely, at electronegative sites the work function is increased, pushing the Fermi energy down and leading to a decrease in neutralization. Thus, the neutralization has a more complex trajectory-dependent behavior when the surface potential is inhomogeneous. In the case of CeO_2, the reduction in neutral fraction as the trajectories become more grazing was ascribed to the local distribution of charge at the surface—the negatively charged oxygen atoms sit higher up at the surface than the positively charged Ce atoms, so that the ions scattered from the Ce sites pass by the electronegative O atoms as they exit the surface at more grazing angles. Hence, the neutralization decreases with angle.

Unlike CeO_2, the positive Bi and negative O surface atoms in BSCCO are nominally at the same height, with at most a small wavy periodicity of 0.03 nm along the c axis.[20] It is then expected that as the emission angle is increased, the ions scattered from Bi would pass near the negatively charged oxygen sites along the outgoing trajectory, but not as close as would an ion scattered from Ce in CeO_2. Consequently, the result for BSCCO should be qualitatively the same as on the ceria surface, but less pronounced, and that is indeed what is seen. In CeO_2, the neutralization probability changed from 100% down to about 40% as the trajectories became more grazing,[19] whereas here the change is more modest, from perhaps 70% to 40%.

IV. ADSORPTION

A. Results

Figure 3 shows the effects that alkali (K) and a halogen (I) adatoms have on the neutralization of Na^+ ions scattered

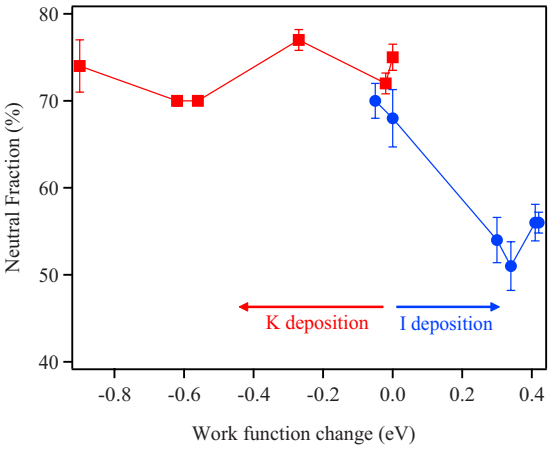

FIG. 3. (Color online) The neutralization of scattered 2 keV Na^+ shown with respect to the work function changes that are induced by adsorption of potassium (positively charged, which decreases the work function) and iodine (negatively charged, which increases the work function).

from the Bi sites into the surface normal direction. The work function is decreased by K adsorption and increased by I, as would be expected from a simple consideration of the charge of the adatom species. Both adsorbates saturate the surface, presumably because there are a limited number of available sites (i.e., they follow the Langmuir model).

Although a large work function change is observed as K is deposited, surprisingly there is no significant change in the scattered Na^+ neutral fraction for scattering from Bi at any K coverage. When I is deposited on the surface, however, the neutralization probability changes significantly with even a small deposition. Taking into account the total adsorbate flux and chamber geometry, it is estimated that for the points with elevated work function, the I_2 exposures are such that each surface atom has been hit by approximately one iodine molecule. With this exposure, the total adatom coverage is likely to be well below 1 ML since the sticking coefficient should be much less than unity.[12] This exposure decreased the neutral fraction from roughly 70% to 50%, which is well outside of the error bars.

Typically, the projectile-surface electronic system can be modeled by assuming that the incoming ionization level is shifted up by an image potential, so that it crosses the Fermi level along the outgoing trajectory. As such, when the work function is significantly altered by the introduction of adsorbates, the neutralization is also strongly affected (at least in the limit of a homogeneous potential), with a negatively charged adsorbate expected to increase the work function and thus decrease the neutralization. To observe any change in work function at all implies that a dipole exists somewhere near the surface, as the otherwise grounded sample has no excess charge. If an adatom adsorbs primarily, or exclusively, to a particular site in the unit cell, the expectation is that the potential will be localized and inhomogeneous. Although the effect of this bonding is reflected in the angular dependence, in trying to determine the local potential the interpretation becomes quite complex. A better way to determine the potential would be to observe how/if the neutralization is altered due to adsorption and compare this to predictions made of the potential for different adsorption scenarios. In the next section we discuss how density functional theory helps explain our findings.

TABLE I. Electrostatic energy associated with the adsorption of atoms for iodine and potassium atoms above a BSCCO surface for various trial sites, as calculated by DFT.

	Iodine	Potassium
	Binding energy (eV)	
Bi top	−0.70	0.40
O top	−0.71	−0.09
Bridge	−1.62	−0.69
Hollow	−1.90	−0.85

B. Density functional theory

The local work function near the surface of BSCCO was obtained by DFT calculations with the Vienna *ab initio* simulation package (VASP) using the generalized gradient approximation and employing the PW91 functional.[21] An energy cutoff of 350 eV was chosen for the basis set and the projector augmented wave pseudopotential was used for the description of electron-ion interactions. A slab model with eight atomic layers in a 3×3 supercell of Bi (rotated 45° from the inset of Fig. 1) was used as the clean surface. The central CuO and CaO layers were fixed at their bulk positions, while the topmost BiO and SrO layers were fully relaxed with the criterion that the maximum force on the atoms must be smaller than 0.01 eV/Å.

Several high-symmetry positions, such as top site, bridge site, and hollow site, were chosen as test sites for the adsorbates, and the crystal was allowed to relax to its lowest-energy arrangement. The resulting binding energies are displayed in Table I. They show that atomic iodine has its lowest energy starting at a hollow site, relaxing to a position with a binding energy of −1.90 eV, while potassium, beginning at the same hollow site, relaxes somewhat far away with a minimum energy of −0.85 eV. After finding the arrangement of least energy, the LEP was calculated with the atom in its fully relaxed position.

The real-space relaxed surface structures that resulted from this calculation are shown in the top panels of Figs. 4 and 5. K significantly perturbs the crystal structure, and is predicted to adsorb nearly on top of an O site somewhat far from the nearest two Bi neighbors. This site would place the positively charged K adatom nearly equidistant from the positively charged Bi sites. Iodine, on the other hand, is expected to adsorb on a hollow site 3 Å above the surface, forming a nearly regular pyramid with the nearest Bi and O. These predictions are consistent with an intuitive chemical picture, since the *p* level of the iodine atom can bond covalently with several sites, while the *s* level of the K would more likely form an ionic bond with O^{2-}.

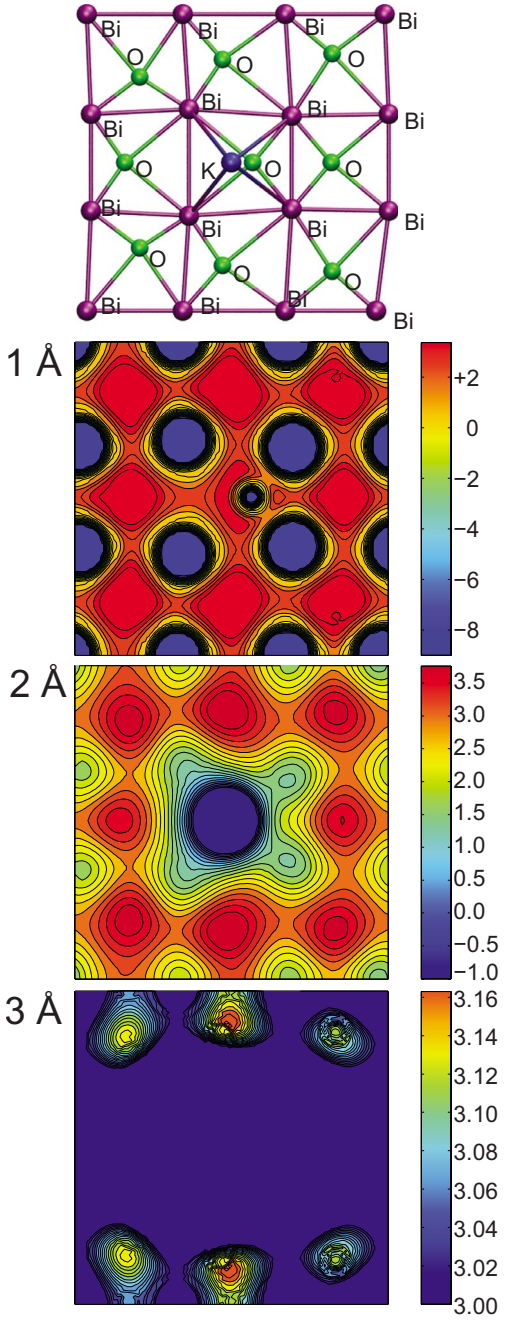

FIG. 4. (Color online) Local work function contour plots of BSCCO surfaces with adsorbed potassium, at 1, 2, and 3 Å from the atomic plane, along with a diagram of the real-space relaxed structure, as calculated by DFT. Each plot is 10 Å square and energy values are given in eV.

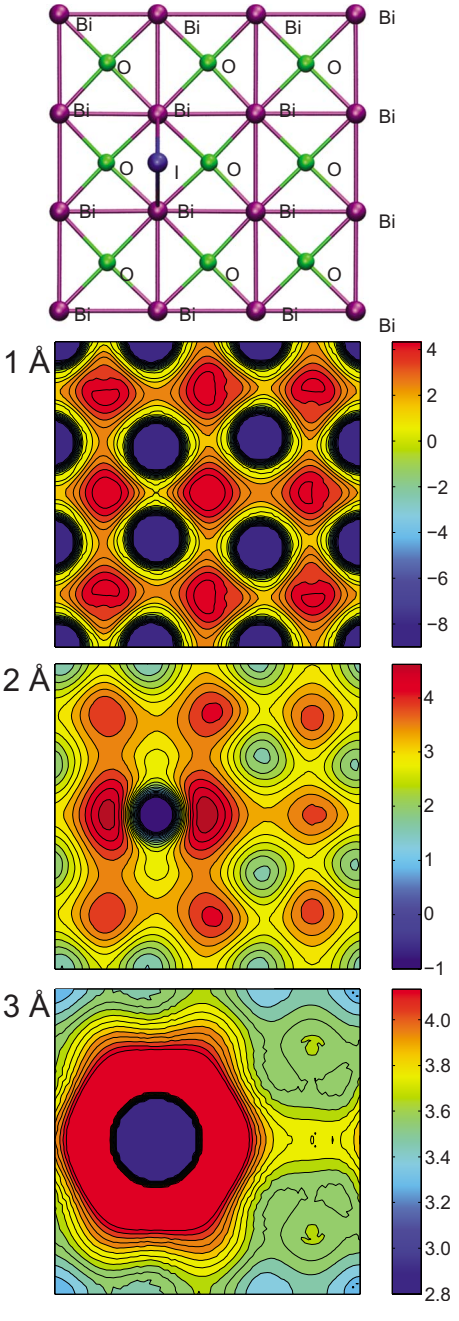

FIG. 5. (Color online) Local work function contour plots of BSCCO surfaces with adsorbed iodine, at 1, 2, and 3 Å from the atomic plane, along with a diagram of the real space relaxed structure, as calculated by DFT. Each plot is 10 Å square and energy values are given in eV.

Contour plots of the calculated local work function for BSCCO with K and I adsorbates are shown in the lower panels of Figs. 4 and 5, at distances of 1, 2, and 3 Å above the plane of the surface Bi atoms. Contour plots at 1 Å show virtually no effect from the adsorbed adatom compared to the clean surface in either case, other than the slightly positive charge induced on the O atom below the K adatom, as the adsorbate attracts the extra electron. Moreover, the calculated Bi energy at 1 Å (a large negative value <-31 eV) would predict no neutralization, as the Fermi level would be so far below the ionization level of the incoming ion that it would be unable to neutralize it from a purely energetic consideration. Similarly, at 3 Å the surface potential is not expected to make a major contribution to the charge exchange, since the potential there appears to be more or less uniform except at the adsorbate site itself, in contradiction with the argument above regarding the angular dependence of neutralization. However, at 2 Å there is both a significant corrugation in the potential, including the expected shift due to the adsorbate, and a reasonable range of energy values to allow for the

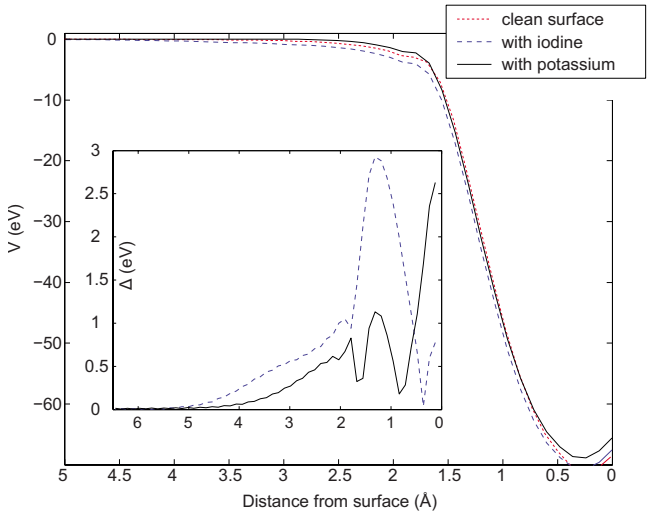

FIG. 6. (Color online) Average LEP above Bi sites as a function of distance from the surface, where the potentials for the clean, iodine-, and potassium-adsorbed surfaces are shown. Inset: the differences between the clean LEP and the iodine-surface and potassium-surface LEP, respectively. The lower curve, corresponding to potassium, shows that, for a certain range of values, the LEP of the potassium-adsorbed surface is considerably closer to that of the clean surface than is the LEP of the iodated surface.

observed neutral fractions. Thus, it could be assumed that the freezing distance for resonant neutralization resides somewhere near 2 Å above the BiO plane in BSCCO.

To more quantitatively determine the freezing distance, the LEP determined by DFT was used to plot the average potential above the Bi sites versus distance from the surface, which is shown in Fig. 6, with the criterion that the potential vanishes at infinity. Note that the distance from the surface is defined here as originating from the mean height of the topmost-layer Bi. The average potential for the iodated surface differs from that of the clean surface for a range of distances, supporting a change in ion neutralization with I coverage. Conversely, for K the potential is rather close to that of the clean surface, suggesting that K adsorption would not lead to a change in neutralization. This is in remarkably good agreement with the measurement, provided that the freezing distance is less than 1.7 Å. Further, since the potential is very large and negative below about 1.5 Å, the freezing distance is likely to be between 1.5 and 1.7 Å. The difference between the adsorbed curves and the clean surface curve is plotted in the inset of Fig. 6, which shows the greatest disparity between the curves between the curves at 1.65 Å. This is a plausible value for the freezing distance at this ion energy.[18]

We note that the prediction is not that the overall work function of the surface does not change upon K adsorption. Indeed, the DFT results do predict that the average overall work function would be altered in the presence of either adsorbate in a manner qualitatively consistent with the measured work function changes. However, since the freezing distance is close to 1.6 Å and since the ion probes the potential around the Bi atoms, the overall work function shift is irrelevant to the resonant-charge transfer for the Bi SSP. We further note that the predicted overall work function estimate from the calculation cannot be compared quantitatively to the experimental value, as the coverage of adatoms in the calculation does not match the experimental situation. We thus confine ourselves only to a discussion of relative changes in the work function.

C. Discussion

I_2 and other halogen molecules often adsorb dissociatively, even at low temperature.[22] For TiO_2, chlorine has been shown to sit on a multicoordinated cation site, preferentially adsorbing at an oxygen vacancy.[23] In our case, the neighboring Bi atoms, which are formally in the 2+ oxidation state, reduce slightly, compared to the stoichiometric surface, in order to accommodate the 1− iodine atom on the hollow site. This would affect the potential at the Bi sites, as predicted by DFT, leading to a decreased neutral fraction, as observed.

The absence of a change in Bi SSP neutral fraction in the presence of K can be attributed to the insensitivity of the LEP above the Bi sites, as predicted by DFT. Other than an LEP effect, however, there are two alternative explanations to the result that ionization is affected by iodine but not potassium. First, it could be that single scattering from Bi is shadowed by the adsorbate, so that one or more of the four surface Bi atoms underneath the adsorbate do not contribute to the measured neutral fraction. Second, it could be that the DFT is not predictive when placing the adsorbate in the high-symmetry site because the actual adsorption sites are instead low-symmetry sites such as step edges and defects. We consider these possibilities in turn.

The notion that the adsorbate prevents ions scattering from Bi atoms below it is doubtful for two reasons. First, the TOF spectra show no significant attenuation of the Bi peak as K is deposited. Second, the results of dynamical scattering simulations performed with KALYPSO (Ref. 24) predict no attenuation of the peak: simulations using the ZBL screened potential tracked a large number of collisions of Na^+ ions with the crystal to determine the kinematics of the backscattered ions. A cell, made of the four atoms with the predicted relaxed locations of the Bi atoms nearest to the K atom, was bombarded by 2 keV Na^+ atoms under conditions identical to the experiment. This simulation showed a strong single-scattering peak in the energy spectrum. When K was added in the predicted adsorption position and the simulation was run again, no significant change of the single-scattering peak intensity was observed, and the only difference in the spectrum was the addition of a very small peak corresponding to Na^+ scattering from K. This suggests that the ions probe all of the Bi atoms in the unit cell regardless of the presence of the K adsorbates. Thus, the calculated average value of the potential at the Bi atoms shown in Fig. 6 is the proper one for comparison to the experimental data, as it includes all atoms in the unit cell.

A more plausible explanation than the shadowing effect is that K adsorbs at sites other than those suggested by the DFT calculation. It has been observed previously (see, e.g., Ref. 25) that alkalis on oxide surfaces can chemisorb at step edges

and crystal defects. This has also been observed for some metal reconstructions.[26] On semiconductor surfaces, adsorbed alkalis can form chains, or "nanowires."[27] Thus, there is a general trend that alkalis often adsorb to form small structures, rather than as isolated adatoms. Although we cannot determine from the present data whether the K is agglomerated at step edges or if it has formed small islands or chains, such adsorption would explain the results. Under this assumption, the saturation coverage could be low and the neutralization in scattering from Bi atoms, the preponderance of which are far away from the K atoms, would be generally unaffected. The adsorption would still influence the macroscopic work function, however, as was observed. STM measurements are suggested as a means for determining the actual adsorption behavior of alkalis on BSCCO.

V. CONCLUSIONS

Low-energy ion scattering is an effective probe of the physical and electronic surface structure of BSCCO-2212, namely the local work function changes and physical reconstruction due to adatom adsorption, when used in conjunction with a DFT analysis. The energetically favored adsorption sites for iodine and potassium influence the average potential around the surface Bi atoms in a manner commensurate with the change in neutralization probability seen in the experiment. In particular, iodine adatoms remove charge from Bi sites, leading to a decrease in the neutral fraction, while K adatoms do not affect the average LEP at the Bi sites. These facts, when considered together, imply that resonant-charge transfer determines the measured neutral fractions, with a characteristic freezing distance of 1.6 ± 0.1 Å.

ACKNOWLEDGMENTS

The authors would like to thank A. N. Pasupathy for his guidance in mounting and cleaving the BSCCO samples and to M. A. Karolewski for his assistance with the scattering simulations. This material is based on work supported by, or in part by, the U.S. Army Research Laboratory and the U.S. Army Research Office under Contract/Grant No. 52723PH. The work at BNL was supported by Department of Energy under contract No. DE-AC0298CH10886.

*Corresponding author; yarmoff@ucr.edu

[1] K. K. Gomes, A. N. Pasupathy, A. Pushp, S. Ono, Y. Ando, and A. Yazdani, Nature (London) **447**, 569 (2007).
[2] K. McElroy, J. Lee, J. A. Slezak, D.-H. Lee, H. Eisaki, S. Uchida, and J. C. Davis, Science **309**, 1048 (2005).
[3] K. Tanaka, W. S. Lee, D. H. Lu, A. Fujimori, T. Fujii, Risdiana, I. Terasaki, D. J. Scalapino, T. P. Devereaux, Z. Hussain, and Z.-X. Shen, Science **314**, 1910 (2006).
[4] S. H. Moffat, R. A. Hughes, G. D. Poulin, J. S. Preston, D. N. Basov, T. Stract, and T. Timusk, IEEE Trans. Appl. Supercond. **7**, 2005 (1997).
[5] A. A. Dzhurakhalov and F. F. Umarov, Nucl. Instrum. Methods Phys. Res. B **171**, 509 (2000).
[6] J. W. Rabalais, *Low Energy Ion-Surface Interactions* (Wiley, New York, 1994).
[7] G. Kimmel and B. Cooper, Rev. Sci. Instrum. **64**, 672 (1993).
[8] J. Los and J. J. C. Geerlings, Phys. Rep. **190**, 133 (1990).
[9] J. Zavadil, Surf. Sci. Lett. **143**, L383 (1984).
[10] C. B. Weare and J. A. Yarmoff, Surf. Sci. **348**, 359 (1996).
[11] R. D. Gann, G. D. Gu, Z. Xu, and J. A. Yarmoff (unpublished).
[12] W. K. Wang, W. C. Simpson, and J. A. Yarmoff, Phys. Rev. B **61**, 2164 (2000).
[13] J. A. Yarmoff and C. B. Weare, Nucl. Instrum. Methods Phys. Res. B **125**, 262 (1997).
[14] Y. Matsui, H. Maeda, Y. Tanaka, and S. Horiuchi, Jpn. J. Appl. Phys. **27**, L372 (1988).
[15] O. S. Oen, Surf. Sci. Lett. **131**, L407 (1983).
[16] J. J. C. Geerlings, L. F. T. Kwakman, and J. Los, Surf. Sci. **184**, 305 (1987).
[17] S. Saito, Y. Uhara, Y. Kogushi, H. Yoshida, S. Isono, H. Yamasaki, H. Murakami, T. Sutou, T. Soumura, and T. Kioka, Phys. Status Solidi **202**, R129 (2005) a.
[18] G. A. Kimmel and B. H. Cooper, Phys. Rev. B **48**, 12164 (1993).
[19] G. F. Liu and J. A. Yarmoff, Surf. Sci. **600**, 2293 (2006).
[20] Y. Matsui, H. Maeda, Y. Tanaka, and S. Horiuchi, Jpn. J. Appl. Phys. **28**, L946 (1989).
[21] G. Kresse and J. Hafner, Phys. Rev. B **47**, 558 (1993).
[22] P. A. Dowben and M. Grunze, Phys. Scr., T **4**, 106 (1983).
[23] U. Diebold, Surf. Sci. Rep. **48**, 53 (2003).
[24] M. A. Karolewski, Nucl. Instrum. Methods Phys. Res. B **230**, 402 (2005).
[25] M. Brause, D. Ochs, J. Gunster, T. Mayer, B. Braun, V. Puchin, W. Maus-Friedricks, and V. Kempter, Surf. Sci. **383**, 216 (1997).
[26] A. Norris and R. McGrath, J. Phys.: Condens. Matter **11**, 9549 (1999).
[27] L. J. Whitman, J. A. Stroscio, R. A. Dragoset, and R. J. Celotta, Phys. Rev. Lett. **66**, 1338 (1991).